Journal of Human Evolution 171 (2022) 103239

Contents lists available at ScienceDirect

Journal of Human Evolution

journal homepage: www.elsevier.com/locate/jhevol

Morphological integration of the hominoid postcranium

Mark A. Conaway [a, b, *], Noreen von Cramon-Taubadel [b]

[a] Department of Ecology, Evolution, and Organismal Biology; Iowa State University, Ames, IA, USA
[b] Buffalo Human Evolutionary Morphology Lab, Department of Anthropology, University at Buffalo, Buffalo, NY, USA

ARTICLE INFO

Article history:
Received 20 August 2021
Accepted 21 July 2022
Available online xxx

Keywords:
Integration coefficient of variation
Cercopithecoids
Shoulder girdle
Pelvic girdle
Covariance
Morphometrics

ABSTRACT

Previous research has suggested that magnitudes of integration may be distinct in the postcranium of hominoids when compared to other primate species. To test this hypothesis, we estimated and compared magnitudes of integration of eight postcranial bones from three-dimensional surface scans for 57 *Hylobates lar*, 58 *Gorilla gorilla*, 60 *Pan troglodytes*, 60 *Homo sapiens*, 60 *Chlorocebus pygerythrus*, and 60 *Macaca fascicularis*. We tested the hypotheses that 1) magnitudes of integration would be distinct in the postcranium of hominoids compared to cercopithecoids, with the explicit prediction that magnitudes of integration would be lower in hominoids than in cercopithecoids, and 2) girdle elements (scapula, os coxa) would have lower magnitudes of integration across all taxa. Integration was quantified using the integration coefficient of variation from interlandmark distances reflecting anatomical and developmental modules defined according to a priori criteria. A resampling protocol was employed to generate distributions of integration values that were then compared statistically using Mann–Whitney U tests with Bonferroni adjustment. Support for hypothesis 1 was mixed: with the exception of *Gorilla*, hominoid taxa were less integrated than the cercopithecoids for all anatomical modules. However, *Homo*, *Gorilla*, and, to a lesser extent, *Pan* showed higher integration than *Hylobates* and the cercopithecoids for homologous limb elements, with magnitudes of integration for both modules being lowest for *Hylobates*. These results generally support the hypothesis of distinct patterns of magnitudes of integration in the hominoid postcranium. The high integration of *Gorilla* may be explained by the effects of overall body size. The results supported the predictions of the second hypothesis. Regardless of taxon, the os coxa and scapula were generally the least integrated skeletal elements, while the femur and radius were the most integrated. The lower integration of the girdle elements suggests that the geometric complexities of particular elements may significantly influence study outcomes.

1. Introduction

Postcranial studies of integration—or the coordinated variation of functionally or developmentally connected phenotypic traits (Olson and Miller, 1958; Wagner, 1984; Hallgrímsson et al., 2009; Klingenberg, 2014; Armbruster et al., 2014)—are uncommon in biological anthropology and evolutionary biology (Esteve-Altava, 2017). Moreover, such studies have generally focused on individual limb length measurements, rather than more detailed measurement systems that capture the three-dimensional (3D) shape in addition to length (though refer to the studies by Fabre et al., 2014; Conaway et al., 2018). Hallgrímsson et al. (2002), in a study on limb development in mice (*Mus musculus*) and rhesus macaques (*Macaca mulatta*), found stronger integration in both taxa between developmentally homologous limb elements (e.g., femur/humerus, tibia/radius, fibula/ulna, etc.) than in elements within limbs. Additionally, Schmidt and Fischer (2009) reported that limb proportions are largely conserved in a large sample of quadrupedal mammals, including several primate species, implying high levels of integration within limbs. However, they also reported slightly more variability in magnitudes of forelimb integration. They suggest that this may be due to the more diverse functional activities of the forelimb (foraging, feeding, infant carrying, etc.), particularly in primates. Slight increases in forelimb integration to accommodate arboreality along with nonlocomotor behaviors have been reported in other primate species as well (Rodman, 1979; Cant, 1988; Conaway et al., 2018). Additionally, Villmoare et al. (2014) found slightly reduced levels of within-limb integration compared with between-limb integration in vertical clinging and leaping strepsirrhines, relative to their more quadrupedal counterparts. Indeed,

* Corresponding author.
E-mail address: markcona@iastate.edu (M.A. Conaway).

https://doi.org/10.1016/j.jhevol.2022.103239
0047-2484/

Fabre et al. (2014) found strong integration in the forelimbs of skunks, raccoons, and weasels, particularly in regions contributing to stability of the elbow joint (i.e., the distal humerus and proximal ulna), suggesting that even a small degree of functional independence of limbs may be detectable via the quantification of magnitudes of integration.

Since even small degrees of functional independence of limbs may be detectable in magnitudes of integration, organisms exhibiting more extreme functional divergence of forelimbs and hind limbs, i.e., brachiation in gibbons or bipedalism in humans, would be expected to exhibit magnitudes of within-limb integration comparable to or even stronger than those among developmentally homologous limb elements (Hallgrímsson et al., 2002). Most importantly, however, in order for a species to diverge away from a state of high integration among developmentally homologous limb elements, strong selection for reduced constraint would be required to overcome this canalizing hurdle (Hallgrímsson et al., 2002). In other words, we should expect to see lower overall integration in the postcranium of mammals whose limbs have diverged functionally to an extreme degree, particularly if the degree or nature of functional independence is variable.

In a study of primate limb proportions, Young et al. (2010) found a significantly reduced level of integration among developmental limb homologs in hominoids when compared to cercopithecoid and platyrrhine taxa. This finding is important because it suggests past selection among extinct hominoids for reduced constraint that may have allowed for the evolution of the diverse locomotor repertoires (including human bipedalism) and ensuing morphological diversity found in apes today (Young, 2006; Young et al., 2010; Pavlicev et al., 2010; Almécija et al., 2015). Indeed, Young et al. (2010) showed that partial correlations among adjacent hindlimb elements in humans (in terms of skeletal element proportions) were strong, whereas suspensory apes showed stronger correlations within forelimb elements. The relatively high integration of limb segments in quadrupedal primates may therefore be maintained to facilitate efficient locomotion on all four limbs, suggesting stabilizing selection for a likely ancestral mammalian condition (Lawler, 2008; Young et al., 2010; Rolian, 2014).

The expectation of low integration of the hominoid postcranium has not been universally corroborated, however. In a study of forelimb and hind limb shape covariance, Tallman (2013) found high covariation in hominoids and fossil hominins, particularly in the distal humerus and femur. Additionally, Marroig and Cheverud (2005) have suggested that decreased constraints on the evolution of limbs in hominoids may, somewhat paradoxically, slow evolutionary change rather than facilitate it. In other words, relaxed constraint may result in responses to selection in directions in morphospace that might otherwise have had little or no response due to higher integration of traits. In any case, the extent to which the findings of Young et al. (2010) are empirically supported when quantifying limb bone form using more complex higher dimension measurement systems (as opposed to measuring limb proportions) is currently unclear.

Indeed, there have been analyses of integration in more complex 3D structures such as the primate pelvis. In a study of crab-eating macaque (*Macaca fascicularis*) postcranial integration, Conaway et al. (2018) found that girdle elements (os coxa, scapula) had significantly lower integration than limb bones. The authors suggest that this may be due to lower redundancy of traits in their resampling protocol for girdle elements, as the sampled traits have a more complex 3D shape than limb bones, which have a simpler shape profile (Conaway et al., 2018). Additionally, previous work by Grabowski et al. (2011) and Grabowski (2013) has shown that the human pelvis is more evolvable, and therefore less integrated than other hominoid species Hansen (2003). Moreover, these results, as well as those presented by Mallard et al. (2017), showed that integration among different parts of the pelvis was low, perhaps as a reflection of constraints due to obstetrics and locomotion on its morphology (Grabowski et al., 2011, Grabowski, 2013).

Here we expand on previous work by quantifying postcranial morphological integration of four hominoid taxa, including anatomically modern humans (*Homo sapiens*), common chimpanzees (*Pan troglodytes*), western lowland gorillas (*Gorilla gorilla*), and lar gibbons (*Hylobates lar*), as well as two cercopithecoid species, crab-eating macaques (*M. fascicularis*) and vervet monkeys (*Chlorocebus pygerythrus*) as outgroups for comparison. We used these data to compare patterns of magnitudes of integration—or the magnitude of integration of a given trait relative to other traits—to address two hypotheses. First, we hypothesized that magnitudes of integration may be distinct in the postcranium of hominoids as compared to other catarrhine species (Hypothesis 1). To test this hypothesis, we made the following two predictions based on previous findings (e.g., Hallgrímsson et al., 2002; Young et al., 2010; Jung et al., 2021):

Prediction 1a: Hominoid taxa will have lower magnitudes of integration for anatomically defined modules relative to the two cercopithecoid taxa.
Prediction 1b: Hominoid taxa will have lower magnitudes of integration for developmentally homologous limb/girdle elements (e.g., femur/humerus etc.) than cercopithecoids.

Second, following Conaway et al. (2018), Grabowski et al. (2011) and Grabowski (2013), we hypothesize that magnitudes of integration of girdle elements (scapula, os coxa) will be lower, on average, than those for long bones in all taxa (Hypothesis 2). Inclusion of multiple taxa in the present study will allow us to test both the methodological suggestion of Conaway et al. (2018) that girdle element integration is affected less by trait redundancy and the biological conclusions of Grabowski et al. (2011), Grabowski (2013) and Mallard et al. (2017), namely, that integration of the human pelvis is low compared to other primates.

Recognizing morphological integration in the skeleton is challenging with simple analyses of trait covariance (Hallgrímsson et al., 2009). The sample analyzed here was selected and constructed to facilitate intertaxonomic analysis within a relatively small but variable clade. To address our hypotheses, similar methods to those utilized in the study by Conaway et al. (2018) were employed, wherein integration of modules, defined a priori based on anatomical and developmental criteria, was calculated using interlandmark distance data and the integration coefficient of variation (ICV; Shirai and Marroig, 2010).

2. Materials and methods

2.1. Sample composition

This study included data obtained from 3D surface scans of adult males and females of four extant hominoid taxa, *H. sapiens* ($n = 60$), *P. troglodytes* ($n = 58$), *G. gorilla* ($n = 58$), and *H. lar* ($n = 55$), and two extant cercopithecoid species, *M. fascicularis* ($n = 60$) and *C. pygerythrus* ($n = 60$; Table 1). Scans were collected from individuals housed at the Cleveland Museum of Natural History, Ohio; the American Museum of Natural History, New York; the Smithsonian National Museum of Natural History, Washington, DC; the Museum of Comparative Zoology, Harvard University, Cambridge, MA; and the University at Buffalo Skeletal Collection, Buffalo, NY. Nonhuman specimens were a mix of wild-shot, zoological, and biomedical individuals. A full list of specimens, including collection, accession number, and provenance is included in

Table 1
Sample breakdown for the present study.

Taxon	Males	Females	Total
Macaca fascicularis	30	30	60
Chlorocebus pygerythrus	30	30	60
Homo sapiens	39	21	60
Pan troglodytes	33	27	60
Gorilla gorilla	38	20	58
Hylobates lar	29	28	55

Supplementary Online Material (SOM) Table S1. Adult status was determined by fully erupted upper and lower third molars and fusion of limb bone epiphyses. Only specimens lacking in obvious pathology of the postcranium were selected for this study. Scans of specimens were chosen with the intent of collecting balanced samples of male and female individuals where available. *Pongo* was excluded from this study because sample sizes were insufficient for reliable calculation of the measure of integration used here (see below).

The rationale for focusing on hominoids was twofold. First, most integration studies of primates have focused on only one or two species (i.e., Hallgrímsson et al., 2002), or if they focus on multiple species, they include only one or two skeletal elements (Grabowski et al., 2011, Grabowski, 2013; also refer to the study by Esteve-Altava, 2017, for a review). Thus, it can be extremely difficult to compare any two given studies. Second, morphological integration has great potential to be used to elucidate taxonomic signals, whether at the subgeneric or suprataxonomic level. In particular, patterns of magnitudes of integration may reflect relationships between skeletal shape and locomotor behaviors (Young et al., 2010; Grabowski et al., 2011; Conaway et al., 2018). Therefore, it was necessary to choose a taxonomic group for which sufficient data could be collected to calculate integration reliably. Although extant Hominoidea is a relatively small taxonomic group and only four taxa are included here, we chose these taxa in an effort to be broadly representative of the locomotor diversity of Hominoidea so that results can be extrapolated more broadly across hominoid taxa.

2.2. Data collection

Three-dimensional surface scans were collected using an HDI-120 surface scanner and its companion software FlexScan 3D v. 3.4.5. Landmark data were collected on 3D surface scans of the os coxa, femur, tibia, fibula, scapula, humerus, radius, and ulna of all taxa. Basic information on the number of landmarks for each skeletal element is provided in SOM Table S2. The landmarking protocols reported here were modified slightly from Conaway et al. (2018) to achieve comparability across all hominoid taxa included in this study. Specifically, some landmarks were removed because they were not visible on hominoid taxa. First, a landmark characterizing the intertrochanteric fossa of the femur was removed because it was not visible on several specimens. Likewise, a landmark on the teres major fossa of the scapula was removed for the present analyses given that the teres major fossa is either absent or very difficult to see in some hominoids. Two landmarks characterizing the deltoid tuberosity and the intertubercular groove of the humerus were not included because they were not apparent enough on the hominoid taxa. Finally, landmarks at the posterolateral point of the radial articular surface of the ulna and the deepest point of the radial notch of the radius were not included. Given these changes, results for *Macaca* in this study may differ slightly from those presented in the study by Conaway et al. (2018).

Intraobserver error was measured for these protocols by Conaway et al. (Conaway et al., 2018) using a method originally developed by von Cramon-Taubadel et al. (2007) and Corner et al. (1992). For each protocol, the standard deviation (in mm) was calculated for three repeats on the same scan. All landmarks were repeatable to within 1 mm. Full descriptions of the landmarking protocols and intraobserver error values can be found in SOM Tables S3–S10 and SOM Figures S1–S8.

Subsets of these landmark data were then used to generate the a priori modules described below. The anatomical modules were made up of the interlandmark data from each skeletal element as a whole (scapula, humerus, radius, ulna, os coxa, femur, tibia, fibula). Developmental modules were created by combining interlandmark data from developmentally homologous skeletal elements: the os coxa and scapula (girdle homolog), humerus and femur (stylopod homolog), tibia and radius (zeugopod homolog 1), and the fibula and ulna (zeugopod homolog 2). Scans were collected as part of a larger project and will be made openly available to researchers upon its completion. Morphometric data are available from the first author upon reasonable request.

2.3. Analyses

Interlandmark distances were calculated using Euclidean Distance Matrix Analysis (Lele and Richtsmeier, 1991), which returns all possible interlandmark distances for a set of landmark data. These analyses were performed using Past3 v. 3.26 (Hammer et al., 2001).

Integration was quantified using the ICV. The ICV is defined as the coefficient of variation of the eigenvalues of covariance matrices and is an adaptation by Shirai and Marroig (2010) of Wagner (1984) and his work with eigenvalue distributions:

$$\mathrm{ICV} = \frac{\sigma(\lambda)}{\bar{\lambda}}$$

Here, $\sigma(\lambda)$ equals the standard deviation of the eigenvalues of a covariance matrix divided by the average of those eigenvalues ($\bar{\lambda}$). The rationale behind the metric is that the distribution of eigenvalues is a reflection of the distribution of variation within a sample (Wagner 1984), which in turn is representative of the magnitude of integration in a sample (Young 2006; Hallgrímsson et al., 2009).

The ICV is sensitive to the number of traits included in the input covariance matrix, as well as the number of specimens being measured (Jung et al., 2020a; SOM Fig. S9). Therefore, trait number must be standardized via a resampling protocol (see below), particularly when analyzing modules with different numbers of landmarks (and therefore different numbers of interlandmark distances). Target sample sizes were based on results of simulation work performed by Jung et al. (2020a), which suggested that a sample >40 is necessary for stable calculation of the ICV (see SOM S1 for more detailed discussion; see also SOM Table S11).

The main utility of the ICV is in intertaxonomic comparisons of integration, and it has been used to that effect by a number of investigators (Shirai and Marroig, 2010; Porto et al., 2013; Garcia et al., 2014; Conaway et al., 2018; Jung et al., 2020b). Shirai and Marroig (2010) concluded that size variation resulting from sexual dimorphism can significantly increase returned integration magnitudes when integration is calculated with the ICV. Additionally, Shirai and Marroig (2010) found that patterns of magnitudes of integration can change and reveal different patterns of modularity when size is removed, although the pattern of magnitudes of integration appears much less variable than the absolute magnitudes. These results have been corroborated in subsequent work using the ICV (Porto et al., 2013; Garcia et al., 2014).

Therefore, prior to analysis, all data were mean standardized (Hansen and Houle, 2008) separately within sexes to adjust for the potential effects of sexual size dimorphism and to correct for large discrepancies in the means and variances of traits across modules. Mean standardization is considered permissible and occasionally even beneficial for data on ratio, log-interval, and interval scales (Hansen and Houle, 2008). Typically, morphometric data, particularly measurements of length (or in this case, interlandmark distances), are considered to be on a ratio or log-interval scale, so mean standardization is permissible given that it does not alter the relationship between two given traits, beyond the necessity of the removal of size difference due to sexual dimorphism (Lande, 1977; Houle, 1992; Hansen and Houle, 2008). Further, this data standardization was necessary given that the ICV is sensitive to large differences in variances among traits, which would cause a disproportionate amount of overall variance to be captured by the first eigenvector, potentially leading to artificially inflated first eigenvalues (and, by extension, inflated ICV values). As shown in SOM Figure S10, for a highly integrated and nonstandardized data matrix, the vast majority of the overall variation (i.e., 60–98%) will be contained within the first eigenvector, generally representative of size (Porto et al., 2009, 2013; Marroig and Cheverud, 2010). As a result, the ICV for the matrix in question (SOM Fig. S10A) will be high despite the fact that a single eigenvector is explaining nearly all of the variance because the difference between the highest and lowest eigenvalues is magnified. In other words, a distinction must be made between statistical variance of individual traits and the dispersion of eigenvalues within a matrix. This effect can, to a certain extent, be mitigated through standardization of data prior to analysis, particularly mean standardization, which removes the effect of large differences due to size without having an effect on the overall variance (Hansen and Houle, 2008; SOM Fig. S10B).

Hence, given the need to resample traits to create sample distributions of covariance matrices (see below), data standardization was necessary to control the disproportionate influence of highly variable traits and to ensure that the results obtained are not simply artifacts of the ICV statistic employed to quantify morphological integration.

Here, for each dataset (that is, each set of interlandmark distances on a skeletal element for a single taxon), each trait, or interlandmark distance, was mean standardized within sex. Specifically, the mean of a given trait (either for males or for females) was subtracted from a single value for that trait for a given individual and then divided by that male or female trait mean. This process was carried out for each individual and subsequently for each trait within a dataset. This process was performed for males and females separately. Again, see SOM Figure S10 for an illustration of the effects of mean standardization on eigenvalue distribution.

The resampling protocol employed here followed that of Conaway et al. (2018), whereby randomly sampled sets of ten interlandmark distances were used to generate a covariance matrix from which the ICV was calculated. This process was then repeated 5000 times for each skeletal element within each taxon to generate distributions of ICV values for subsequent statistical comparison. The importance of this protocol is to allow for statistical comparison of ICV values among elements that have been characterized with different numbers of traits.

After resampling and ICV calculation, the resulting distributions of ICV values were compared using pairwise Mann–Whitney U tests with Bonferroni correction for multiple comparisons ($\alpha = 0.0025$), both within skeletal modules and across taxa (to test the predictions of Hypothesis 1), as well as within taxa and across skeletal elements (to test Hypothesis 2).

3. Results

3.1. Intertaxonomic results

The ICV results for the anatomical modules for each taxon are reported in Table 2, and results of all pairwise Mann–Whitney U tests for intertaxonomic differences can be found in the SOM Tables S12–S19. In terms of overall integration of anatomically defined modules, *P. troglodytes* and *H. lar* were significantly less integrated ($p < 0.0025$) than the two cercopithecoid taxa included here (Fig. 1; Table 2; SOM Tables S12–S19). Humans generally followed *Pan* and *Hylobates* in exhibiting lower integration for the anatomical modules than the cercopithecoids, with the exception of the ulna, tibia, and radius, which were more strongly integrated in at least one of the two cercopithecoid taxa. However, with the exception of the scapula (Table 2), all anatomical modules were significantly ($p < 0.0025$) more integrated in *G. gorilla* than in the other hominoid and cercopithecoid taxa (Table 2; SOM Tables S12–S19).

A similar pattern of integration was observed for the developmental modules, with some exceptions (Fig. 2; Table 3; see also SOM Tables S20–S23). In general, *P. troglodytes* and *H. lar* were significantly less integrated ($p < 0.0025$) than the two cercopithecoid taxa, with the exception of the zeugopod homolog 1 (tibia + radius) for *P. troglodytes*, which showed a slightly elevated integration statistically equivalent to that found for *Macaca* and significantly higher than that found for *Chlorocebus* (Table 3; SOM Table S22). Compared to the cercopithecoids, *G. gorilla* showed significantly higher integration values across all developmental modules (Table 3; SOM Tables S20–S23), while humans showed significantly higher integration values for all developmental modules except the girdle module (Table 3; SOM Table S20).

3.2. Integration of anatomical and developmental modules

Figure 3 depicts distributions of ICV values for the anatomical modules of all taxa. With some exceptions (described below), Mann–Whitney U tests show that comparisons of anatomical modules were significantly different among modules within each taxon (SOM Tables S24-S29). Likewise, with a few exceptions, girdle elements were significantly less integrated than limb elements for all taxa. Finally, the rank order of ICV values for anatomical elements was largely preserved across taxa.

For *Macaca*, the fibula, scapula, and os coxa were statistically equivalent in terms of their comparatively low magnitudes of integration (Table 2; SOM Table S24). In *Homo*, the ulna and femur were statistically equivalent in average magnitudes of integration (Fig. 3; Table 2; SOM Table S26). In *Gorilla*, the humerus and femur were statistically equivalent to each other in average magnitudes of integration (Table 2; SOM Table S28). The humerus and femur of *Hylobates* were found to be statistically equivalent, as well as the ulna and the fibula in terms of their average magnitudes of integration (SOM Table S29). The overall pattern of magnitudes of ICV values for *Hylobates* differed from the other taxa in that the scapula and ulna were the least integrated, whereas the os coxa was more comparable to the tibia and femur in terms of integration.

Figure 4 depicts distributions of ICV values of developmental modules for all taxa. As with the anatomical modules, the developmental module comprised of girdle elements (Girdle Homolog) was generally significantly less integrated than the other developmental modules, with the exception of *Hylobates* (Fig. 2; SOM Tables S30–S35). The rank order of the remaining developmental modules for each taxon was less consistent than that seen for the anatomical modules. The stylopod homolog was most integrated for *Chlorocebus*, zeugopod homolog 1 was most integrated for *Homo, Pan*, and *Macaca*, and finally, zeugopod homolog 2 was most

Table 2
Mean integration coefficient of variation for anatomical modules across all taxa.

	Os coxa	Femur	Tibia	Fibula	Scapula	Humerus	Radius	Ulna
Macaca fascicularis	1.98	2.18	2.07	1.99	1.97	2.17	2.14	2.05
Chlorocebus pygerythrus	1.69	2.29	1.93	1.81	1.67	2.14	2.15	1.85
Homo sapiens	1.51	1.96	1.99	1.68	1.63	2.11	2.17	1.95
Pan troglodytes	1.48	1.89	1.80	1.72	1.53	1.87	1.84	1.62
Gorilla gorilla	2.07	2.51	2.27	2.13	1.64	2.49	2.64	2.37
Hylobates lar	1.61	1.66	1.55	1.48	1.43	1.66	1.68	1.48

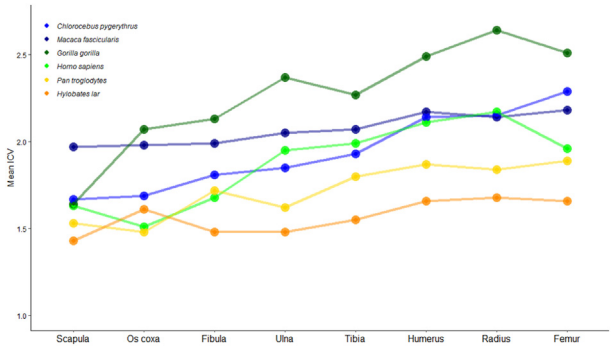

Figure 1. Mean integration coefficient of variation (ICV) of anatomical modules for each taxon. With the exception of *Gorilla*, the mean ICVs for each skeletal element of the hominoid taxa are generally lower that those of the cercopithecoid taxa.

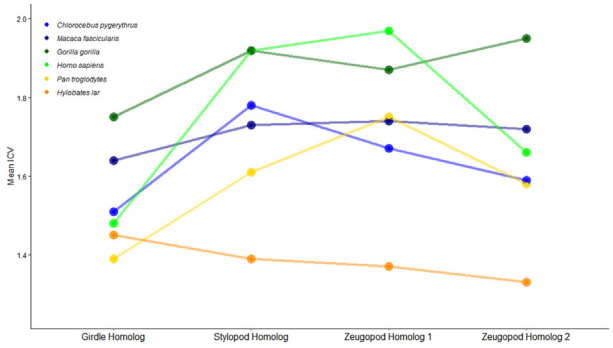

Figure 2. Mean integration coefficient of variation (ICV) of developmental modules for each taxon. Overall, the magnitudes of ICV values of hominoids are comparable to those of cercopithecoids, with the exception of *Hylobates*, which shows overall lower magnitudes of integration.

integrated for *Gorilla*. After Bonferroni correction, the zeugopod 1 and stylopod homolog modules were statistically equivalent for *Hylobates*.

4. Discussion

Here we tested two hypotheses related to morphological integration of the hominoid and cercopithecoid postcranium. The first hypothesis was that patterns of magnitudes of integration in the postcranium of hominoids would be distinct compared to cercopithecoids. Based on previous research, we predicted that hominoid taxa would present with overall lower levels of integration in 1) anatomical and 2) developmentally defined postcranial modules than the cercopithecoid outgroups. However, these predictions were only partially supported. While lower levels of integration were generally found for *Homo*, *Pan*, and *Hylobates* across anatomically defined modules (Fig. 1; Table 2), with the exception of the scapula, *Gorilla* presented with ICV values that were significantly higher than those of *Macaca* and *Chlorocebus*. In the case of developmental modules, contrary to expectations, humans displayed high integration values for the limb homologs compared with other taxa. Nevertheless, given these results, some general taxonomic patterns can be identified and are elaborated on further below. The second hypothesis that girdle elements would present with lower ICV values than long bones (Conaway et al., 2018) was supported, with the exception of the os coxa and girdle homolog modules of *Hylobates* (Fig. 4; Table 3). Therefore, across all taxa, the scapula was found to be significantly less integrated than limb bones, and the same was found to be true for the os coxa in all taxa except for *Hylobates*.

While *Macaca* and *Chlorocebus* were generally found to be more integrated than the hominoids across the majority of modules tested, the two taxa were found to be just as different from each other, both in terms of absolute magnitude of integration as well as the pattern of magnitudes of integration. This may come down to an issue of sample construction. As shown in SOM Table S1, the sample of macaques studied here are biomedical in origin. Differences in skeletal morphology between captive and wild individuals have been well documented in primates (e.g., Hlusko and Mahaney, 2007; Bello-Hellegouarch et al., 2013) and other mammals (e.g., O'Regan and Kitchener, 2005; Hartstone-Rose et al., 2014), as well as in reptiles (e.g., Drumheller et al., 2016). Further, Corruccini and Beecher (1984) examined the effect of captivity on the craniofacial integration of adult male captive yellow baboons (*Papio cynocephalus*) and found that, overall, the captive individuals presented with lower levels of integration. Likewise, in a preliminary study conducted by the authors, significant differences were found in ICV values for captive and wild crab-eating macaques (*M. fascicularis*; Conaway et al., 2020). The directions of these differences were variable; the captive individuals frequently presented with higher levels of postcranial integration than the wild individuals. Further study is required to understand the full effects of captivity on postcranial integration; however, any differences in integration values between our samples of *Macaca* and *Chlorocebus* might potentially

Table 3
Mean integration coefficient of variation for developmental modules across all taxa.

	Girdle homolog	Stylopod homolog	Zeugopod homolog 1	Zeugopod homolog 2
Macaca fascicularis	1.64	1.73	1.74	1.72
Chlorocebus pygerythrus	1.51	1.78	1.67	1.59
Homo sapiens	1.48	1.92	1.97	1.66
Pan troglodytes	1.39	1.61	1.75	1.58
Gorilla gorilla	1.75	1.92	1.87	1.95
Hylobates lar	1.45	1.39	1.37	1.33

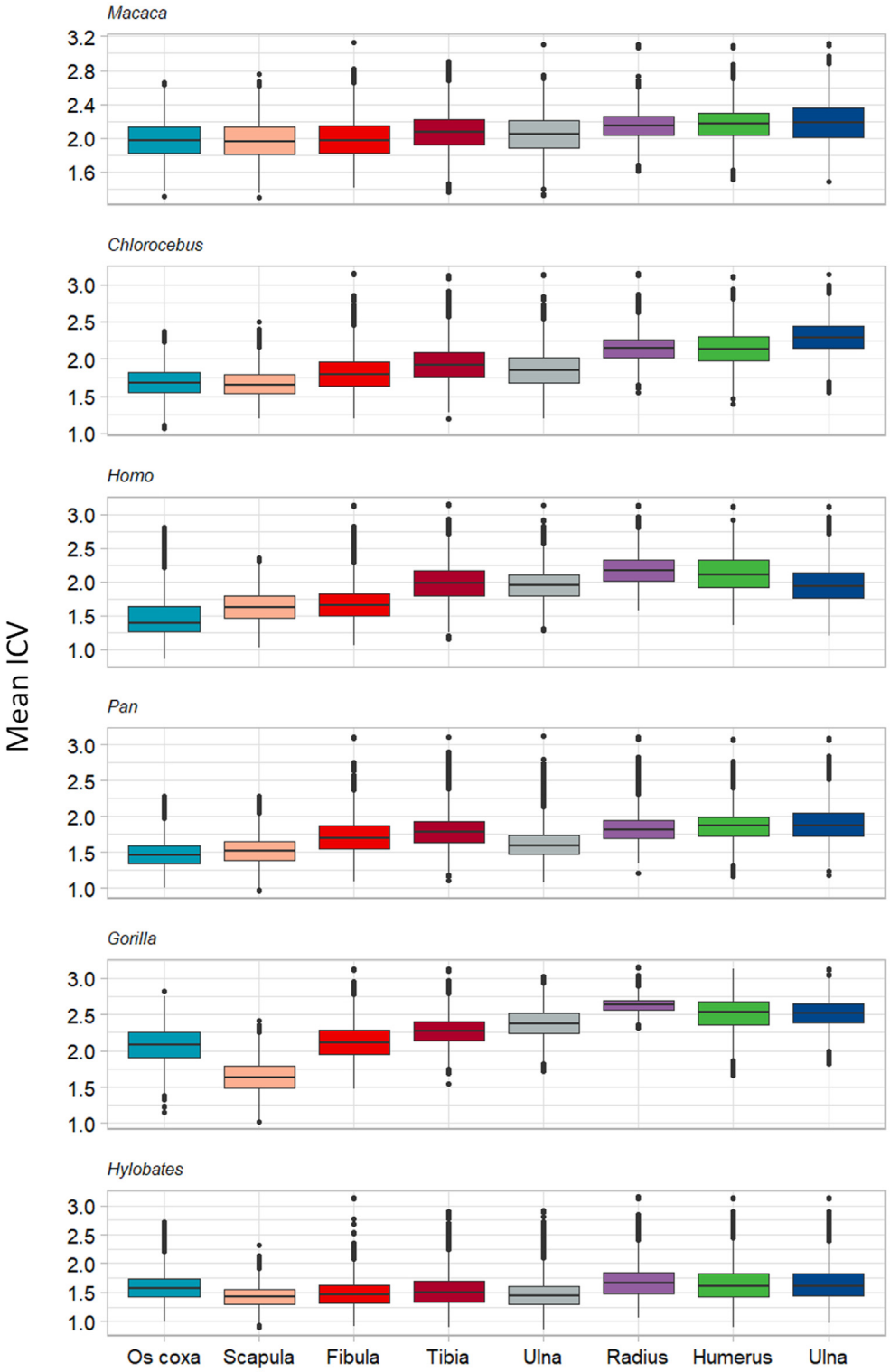

Figure 3. Boxplots showing distributions of the integration coefficient of variation (ICV) for the anatomical modules for each taxon. The center horizontal line of each box represents the median and the interquartile range is represented by the whiskers. Points outside the interquartile ranges represent outlying values. The os coxa and scapula are generally less integrated than the limb bone modules for each taxon.

be explained by morphological variation due to a captive rearing environment.

In terms of magnitudes of integration, humans are generally less integrated than the cercopithecoid taxa (Tables 2 and 3), as expected based on the work of Young et al. (2010). The result for the os coxa is consistent with that of work by Grabowski et al. (2011) and Grabowski (2013) where the human os coxa was found to be significantly less integrated, and therefore more evolvable, than chimpanzees and gorillas. The conclusion drawn by the authors was that this was in response to selection for bipedal locomotion

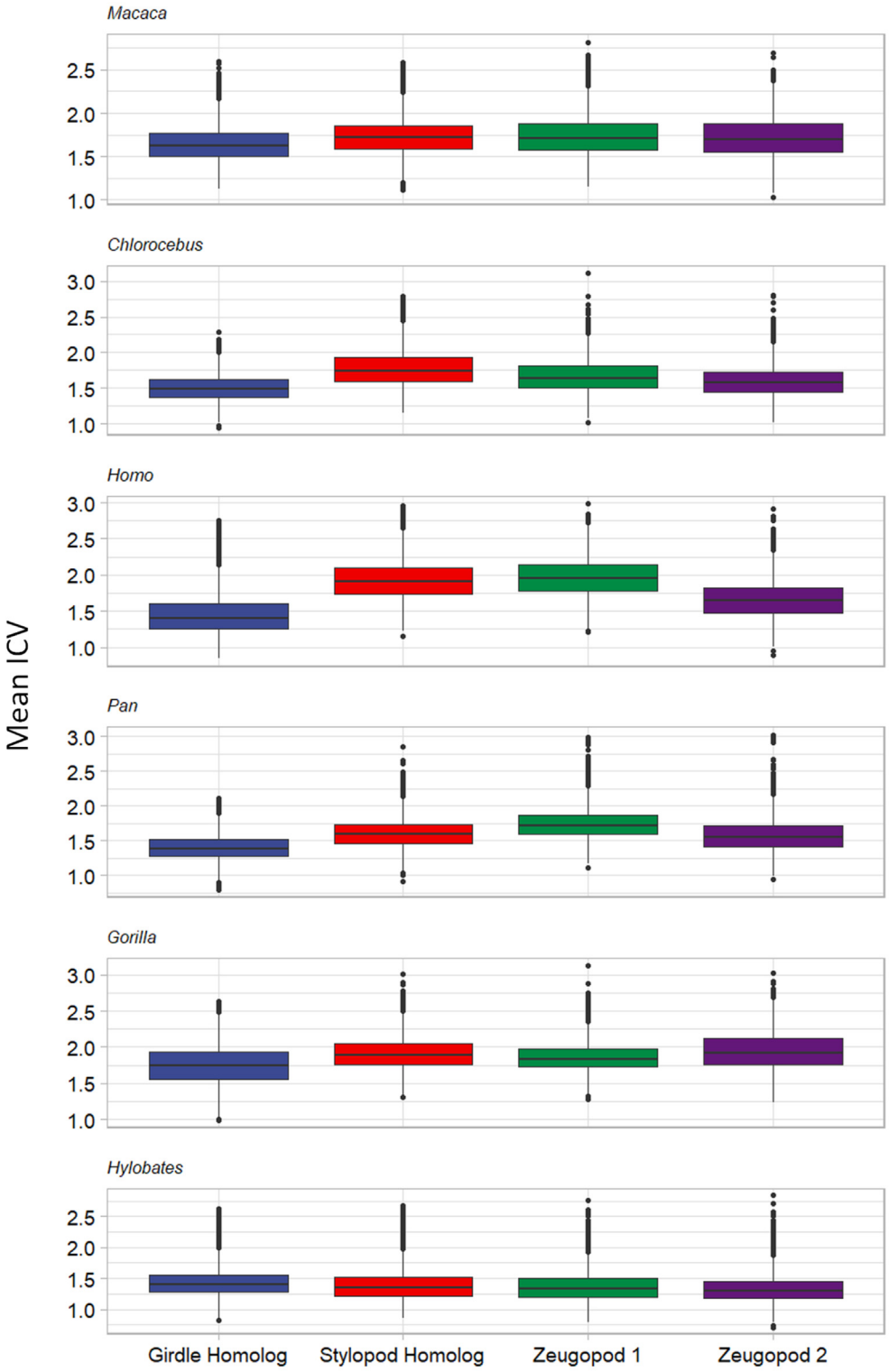

Figure 4. Boxplots showing distributions of the integration coefficient of variation (ICV) for the developmental modules for each taxon. The center horizontal line of each box represents the median, and the interquartile range is represented by the whiskers. Points outside the interquartile ranges represent outlying values. The girdle homolog module is generally less integrated than the other modules for each taxon.

and was a reflection of the overall low levels of constraint in hominoids writ large (Young et al., 2010; Grabowski et al., 2011). The low ICV of the girdle homolog module found here further corroborates this notion, indicating an evolutionary 'decoupling' of the os coxa and scapula. Further, this reduced constraint is hypothesized to have been instrumental in allowing for response to selection pressures for parturition of large-brained infants (Lovejoy, 2005; Grabowski, 2013).

Overall, postcranial integration of *Pan*, in terms of absolute magnitudes, is comparable to that of *Hylobates*, as has also been

shown previously (Young et al., 2010). However, patterns of magnitudes of chimpanzee integration are more similar to those of humans and gorillas. Further, similarly to humans, the Girdle Homolog of *Pan* was among the least integrated modules, which is likewise consistent with previous work (Lewton, 2012; Fig. 4).

While the patterns of magnitudes of integration of the chimpanzee and gorilla are similar to those of humans in some ways, the practical effects of these associations are likely different from a biomechanical perspective. For instance, chimpanzees and gorillas appear very similar to the quadrupedal cercopithecoid taxa in terms of the high integration of the stylopod homolog. Chimpanzees and, to a lesser extent, gorillas exhibit skeletal adaptations of the upper limb and shoulder for suspensory behavior (Young, 2003; Selby and Lovejoy, 2017). However, in practice, both species engage in a far greater proportion of terrestrial quadrupedal knuckle-walking and exhibit skeletal adaptations of the middle phalanges of digits II–V in order to accommodate it (Tuttle and Basmanjian, 1974). This, combined with similarities to the cercopithecoid taxa presented here, suggest that the high integration of the chimpanzee and gorilla forelimb may have the practical effect of facilitating quadrupedal locomotion.

The gibbon is the most distinct among all taxa studied here in terms of both magnitude and pattern of magnitudes of integration. This is perhaps unsurprising given the uniqueness of the hylobatid skeletal morphology relative to other hominoids (e.g., Holliday and Friedl, 2013) as well as its suspensory locomotor behavior and ricochetal mode of brachiation (Larson, 1988; Hunt et al., 1996). In the context of the present analyses, *Hylobates* is distinct in several ways. First, it is on average the least integrated of the taxa analyzed (Figs. 3 and 4; Young et al., 2010). This fact is critical in the interpretation of the pattern of magnitudes of *Hylobates*. Most surprising, however, was that the girdle homolog was the most integrated developmental module and indeed was on par with the anatomical modules, whereas in other taxa, this was among the least integrated modules (Fig. 4). Further research will be required in order to determine exactly why this is the case. However, these results may be explained along the lines of the relatively derived locomotor morphology of *Hylobates*, resulting from an evolutionary relaxation of morphological constraint (Larson, 1998; Young, 2003). When integration is concentrated in specific directions in shape space (modules), the regions outside those directions will have less variation and will channel evolutionary change in those directions of 'genetic least resistance,' often through increases or decreases in relative size (Shirai and Marroig 2010; Klingenberg 2014; but refer to the study by Simons et al., 2020 for an alternative perspective). Therefore, when constraint is reduced, morphological change is permitted in directions in morphospace that would not previously have taken place.

The unexpectedly high integration values for *Gorilla* may be explained by several factors, including the disproportionate effects of scaling for size variation and the landmarking protocols used, in addition to scale effects of covariance matrices. As mentioned above, all interlandmark data were mean standardized within sex. While there are few studies to compare these results to directly, Young et al. (2010) found that *Gorilla* limb proportions were weakly integrated, similar to other hominoid taxa in their study. Their approach to correcting for size was to center their data whereby "differences in means were added to individual values from the group with the lower mean," (Young et al., 2010:3404). Given the similarity between our two approaches for standardizing size, this is likely not the explanation for the unexpectedly high ICV values found here for *Gorilla*. Shirai and Marroig (2010), on the other hand, removed size variation entirely in one of their analyses and found that both the neotropical primates and opossums in their sample became much more similar to each other in terms of magnitudes of integration.

While the mean standardization method that we employed here removes the effects of allometric size differences due to sexual dimorphism (Conaway et al., 2018), size as a factor of covariance (and therefore integration) is not removed. Therefore, size itself may also play a role in the higher ICV values for *Gorilla* since larger organisms tend to have higher covariances and variances (Shirai and Marroig, 2010).

To explore this possible effect, we performed a post hoc analysis on a subset of results where interlandmark data were mean standardized within species as opposed to within sex. The same method as outlined above was employed, whereby mean standardization was performed on each trait. However, each trait was standardized by the species mean for that trait, rather than the within-sex mean. The methodological consequence of this is that all taxa are made to be the same size. Results of this alternate analysis are shown in SOM Figure S11 and illustrate two main points: 1) while in our original analysis the scapula and os coxa were generally the least integrated skeletal elements for all taxa examined, with size removed, they become the most integrated, and 2) differences in magnitudes of integration among taxa are greatly reduced when taxonomic size differences are removed. Crucially, while the magnitudes of integration of the girdles are slightly lower when mean standardized within taxa vs. within sexes, they are still comparable to those shown in the main analyses. In contrast, the effects of mean standardizing by taxon are much more dramatic for the long bones, which all show much reduced ICV values following this method of size adjustment. This suggests that for all taxa, size was an important contributing factor to the integration of long bones, but not necessarily girdle elements. Further, and perhaps most importantly, these results suggest that size was indeed an important distinguishing factor in magnitudes of integration across taxa. Therefore, we argue that, in this case, total removal of all size variation may not be appropriate. While many researchers view size, quite rightly, as a confounding factor in geometric morphometric analyses, it is important to recognize that size itself can be an important factor in generating patterns and magnitudes of integration (Marroig and Cheverud, 2010; Shirai and Marroig, 2010; Grabowski et al., 2011). What this suggests is that for some taxa, size should be included in analyses of magnitudes of integration for interspecific comparisons to be of any use, at least with the current methodology. While the high integration of *Gorilla* is contrary to previous research, it may be due to differences in landmarking protocols. Specifically, previous studies on this subject have utilized measures of limb length, whereas we have included more detailed measurements of the shape of epiphyses. While these concerns add further to the list of theoretical and methodological challenges associated with the study of integration, further work in this regard is beyond the scope of this paper and should be left to future research.

Developmental modules of *Pan* and *Hylobates* were generally lower than that of the cercopithecoids (Table 3). As was the case for the anatomical modules, integration of the developmental modules was highest for *Gorilla*. Likewise, the integration of the Stylopod and Zeugopod 1 homologs of *Homo* were comparable to *Gorilla* in terms of integration. These results run largely counter to expectations. However, it should be noted that previous research, namely by Young et al. (2010), utilized measurements of limb proportions, rather than the more multidimensional measurements utilized here. Therefore, it is possible that characterization of the epiphyses of long bones has introduced previously unknown sources of limb integration. Additionally, the relatively low integration of the Girdle Homolog for *Pan, Hylobates*, but most especially, *Homo*, relative to

the cercopithecoids, is consistent with previous research on scapular and pelvic development (Young et al., 2010; Sears et al., 2015; Agosto and Auerbach, 2021). Though closely related, chimp and human pelvic morphology is very different, whereas the chimp and gibbon are more morphologically similar despite more distant ancestry (Lovejoy, 1988; Sockol et al., 2007; Roach et al., 2013). This suggests that, thanks to a reduction in morphological constraint, a response to selective pressures for bipedalism in humans was possible (resulting in a derived morphology of the pelvis, relative to other hominoids; Grabowski et al., 2011), along with a response to a selective pressure for brachiation in gibbons, resulting in relatively primitive morphology of the hylobatid pelvis.

Our finding that girdle elements generally present lower overall integration than limb elements (Hypothesis 2) could be indicative of an anthropoid primate-wide pattern of magnitudes of integration wherein the pelvic girdle is generally less integrated in all primate species. However, to confirm this, a much broader intertaxonomic study—including strepsirrhine and nonprimate species—is necessary. Studies of integration and/or modularity of the primate pelvic girdle have tended to focus exclusively on humans (Grabowski et al., 2011; Grabowski, 2013; Esteve-Altava, 2017). However, a recent study (Agosto and Auerbach, 2021) focusing on the evolvability of the basicranium and girdle complexes of *Colobus* found strong covariance between the shoulder and pelvic girdles.

5. Conclusions

In this study we compared magnitudes of integration of eight anatomical and four developmental modules in the postcranium of hominoids. Our first hypothesis, that magnitudes of integration in the postcranium would be distinct for hominoids compared to cercopithecoids, had two associated predictions. The prediction that hominoids would present lower integration values than cercopithecoids in both anatomical and developmental modules was only partially confirmed, possibly due to the confounding effects of body size in *Gorilla*. Overall, the hominoid taxa presented with lower average integration relative to the cercopithecoids despite this potential confound. Our second hypothesis, that magnitudes of integration for girdle elements would be lower on average than those of the long bones, was largely supported, with the exception of the results for *Hylobates*. This finding provides partial support for the notion that more complex structures—or at least, structures characterized with more spatially complex landmarking protocols—may be less prone to artificially inflated ICV values. However, further research with even more complex landmarking protocols (that is, those incorporating sliding semilandmarks) will be necessary to determine the extent to which landmarking has an effect on integration results.

Results of this study suggest that a deeper investigation into the qualities of the ICV and of eigenvalue-dispersion-based integration statistics in general is necessary to understand how best to quantify integration magnitudes since little has been done in this arena. Finally, the use of interlandmark distances and a resampling protocol for analyses was based on the need for an avenue for statistical comparison of ICV values of skeletal elements that were characterized with different numbers of landmarks. As results showed a persistent effect of inflated ICV values for long bones relative to girdle elements, future studies of integration using eigenvalue-based statistics like the ICV should explore the effects of different treatments of these data.

Declaration of competing interest

None.

Acknowledgments

We thank the Editor-in-Chief, Associate Editor, and two anonymous reviewers for constructive comments that greatly improved our manuscript. We are grateful to Yohannes Haile-Selassie at the Cleveland Museum of Natural History, Darrin Lunde at the Smithsonian Museum of Natural History, Lawrence Heaney at the Field Museum of Natural History, Mark Omura at the Museum of Comparative Zoology at Harvard University, and staff at the American Museum of Natural History, for granting access to skeletal collections. We thank the SUNY Reuter Foundation for funding to support this research. This research is based upon work supported by a Leakey Foundation Research Grant, as well as the National Science Foundation under grant number BCS-1830745, and the Mark Diamond Research Fund of the Graduate Student Association at the University at Buffalo, State University of New York, United States.

Author contributions

M.A.C.: Conceptualization, data curation, formal analysis, investigation, visualization, writing original draft, and funding. N.v.C.-T.: Conceptualization, investigation, supervision, and funding. Both authors contributed critically to the drafts and gave final approval for publication.

Supplementary Online Material

Supplementary online material related to this article can be found at https://doi.org/10.1016/j.jhevol.2022.103239.

References

Agosto, E.R., Auerbach, B.M., 2021. Evolvability and constraint in the primate basicranium, shoulder, and hip, and the importance of multi-trait evolution. Evol. Biol. 48, 221–232.
Almécija, S., Smaers, J.B., Jungers, W.L., 2015. The evolution of human and ape hand proportions. Nat. Commun. 6, 7717.
Armbruster, S.W., Pélabon, C., Bolstad, G.H., Hansen, T.F., 2014. Integrated phenotypes: Understanding trait covariation in plants and animals. Philos. Trans. R. Soc. B Biol. Sci. 369, 20130245.
Bello-Hellegouarch, G., Potau, J.M., Arias-Martorell, J., Pastor, J.F., Pérez-Pérez, A., 2013. A comparison of qualitative and quantitative methodological approaches to characterizing the dorsal side of the scapula in hominoidea and its relationship to locomotion. Int. J. Primatol. 34, 315–336.
Cant, J., 1988. Positional behavior of long-tailed macaques (*Macaca fascicularis*) in northern Sumatra. Am. J. Phys. Anthropol. 76, 29–37.
Conaway, M.A., Schroeder, L., von Cramon-Taubadel, N., 2018. Morphological integration of anatomical, developmental, and functional postcranial modules in the crab-eating macaque (*Macaca fascicularis*). Am. J. Phys. Anthropol. 166, 661–670.
Conaway, M.A., Kenyon-Flatt, B., von Cramon-Taubadel, N., 2020. A geometric morphometric comparison of shape and integration indices in captive and wild *Macaca fascicularis*. Am. J. Phys. Anthropol. 171, 56–57.
Corner, B.D., Lele, S., Richtsmeier, J.T., 1992. Measuring precision of three-dimensional landmark data. J. Quant. Anthropol. 3, 347–359.
Corruccini, R.S., Beecher, R.M., 1984. Occlusofacial morphological integration lowered in baboons raised on soft diet. J. Craniofac. Genet. Dev. Biol. 4, 135–142.
Drumheller, S.K., Wilberg, E.W., Sadleir, R.W., 2016. The utility of captive animals in actualistic research: A geometric morphometric exploration of the tooth row of *Alligator mississippiensis* suggesting ecophenotypic influences and functional constraints. J. Morphol. 277, 866–878.
Esteve-Altava, B., 2017. In search of morphological modules: A systematic review. Biol. Rev. 92, 1332–1347.
Fabre, A.C., Goswami, A., Peigné, S., Cornette, R., 2014. Morphological integration in the forelimb of musteloid carnivorans. J. Anat. 225, 19–30.
Garcia, G., Cerqueira, R., Hingst-Zaher, E., Marroig, G., 2014. Quantitative genetics and modularity in cranial and mandibular morphology of *Calomys expulsus*. Evol. Biol. 41, 619–636.
Grabowski, M.W., 2013. Hominin obstetrics and the evolution of constraints. Evol. Biol. 40, 57–75.
Grabowski, M.W., Polk, J.D., Roseman, C.C., 2011. Divergent patterns of integration and reduced constraint in the human hip and the origins of bipedalism. Evolution 65, 1336–1356.

Hallgrímsson, B., Willmore, K., Hall, B.K., 2002. Canalization, developmental stability, and morphological integration in primate limbs. Yearbk. Phys. Anthropol. 45, 131–158.
Hallgrímsson, B., Jamniczky, H., Young, N.M., Rolian, C., Parsons, T.E., Boughner, J.C., Marcucio, R.S., 2009. Deciphering the palimpsest: Studying the relationship between morphological integration and phenotypic covariation. Evol. Biol. 36, 355–376.
Hammer, Ø., Harper, D.A.T., Ryan, P.D., 2001. PAST: Paleontological statistics software package for education and data analysis. Palaeontol. Electron. 4, 4.
Hansen, T.F., 2003. Is modularity necessary for evolvability? Remarks on the relationship between pleiotropy and evolvability. Biosystems 69, 83–94.
Hansen, T.F., Houle, D., 2008. Measuring and comparing evolvability and constraint in multivariate characters. J. Evol. Biol. 21, 1201–1219.
Hartstone-Rose, A., Selvey, H., Villari, J.R., Atwell, M., Schmidt, T., 2014. The three-dimensional morphological effects of captivity. PLoS One 9, e113437.
Hlusko, L.J., Mahaney, M.C., 2007. A multivariate comparison of dental variation in wild and captive populations of baboons (*Papio hamadryas*). Arch. Oral Biol. 52, 195–200.
Holliday, T.W., Friedl, L., 2013. Hominoid humeral morphology: 3D morphometric analysis. Am. J. Phys. Anthropol. 152, 506–515.
Houle, D., 1992. Comparing evolvability and variability of quantitative traits. Genetics 130, 195–204.
Hunt, K.D., Cant, J.G.H., Gebo, D.L., Rose, M.D., Walker, S.E., Youlatos, D., 1996. Standardized descriptions of primate locomotor and postural modes. Primates 37, 363–387.
Jung, H., Conaway, M.A., von Cramon-Taubadel, N., 2020a. Examination of sample size determination in integration studies based on the Integration Coefficient of Variation (ICV). Evol. Biol. 47, 293–307.
Jung, H., Simons, E., von Cramon-Taubadel, N., 2020b. Ontogenetic changes in magnitudes of integration in the macaque skull. Am. J. Phys. Anthropol. 174, 76–88.
Jung, H., Simons, E., von Cramon-Taubadel, N., 2021. Examination of magnitudes of integration in the catarrhine vertebral column. J. Hum. Evol. 156.
Klingenberg, C.P., 2014. Studying morphological integration and modularity at multiple levels: Concepts and analysis. Philos. Trans. R. Soc. B Biol. Sci. 369, 20130249.
Lande, R., 1977. On comparing coefficients of variation. Syst. Zool. 26, 214–217.
Larson, S.G., 1988. Subscapularis function in gibbons and chimpanzees: Implications for interpretation of humeral head torsion in hominoids. Am. J. Phys. Anthropol. 76, 449–462.
Larson, S.G., 1998. Parallel evolution in the hominoid trunk and forelimb. Evol. Anthropol. 6, 87–99.
Lawler, R.R., 2008. Morphological integration and natural selection in the postcranium of wild Verreaux's Sifaka (*Propithecus verreauxi verreauxi*). Am. J. Phys. Anthropol. 136, 204–213.
Lele, S., Richtsmeier, J.T., 1991. Euclidean distance matrix analysis: A coordinate-free approach for comparing biological shapes using landmark data. Am. J. Phys. Anthropol. 86, 415–427.
Lewton, K.L., 2012. Evolvability of the primate pelvic girdle. Evol. Biol. 39, 126–139.
Lovejoy, C.O., 1988. Evolution of human walking. Sci. Am. 259, 118–125.
Lovejoy, C.O., 2005. The natural history of human gait and posture. Part 1. Spine and pelvis. Gait Posture 21, 95–112.
Mallard, A.M, Savell, K.R.R, Auerbach, B.M., 2017. Morphological integration of the human pelvis with respect to age and sex. Anat. Rec. 300, 666–674.
Marroig, G., Cheverud, J.M., 2005. Size as a line of least evolutionary resistance: Diet and adaptive morphological radiation in new world monkeys. Evolution 59, 1128–1142.
Marroig, G., Cheverud, J.M., 2010. Size as a line of least resistance II: Direct selection on size or correlated response due to constraints? Evolution 64, 1470–1488.
Olson, E.C., Miller, R.L., 1958. Morphological Integration. University of Chicago Press, Chicago.
O'Regan, H.J., Kitchener, A.C., 2005. The effects of captivity on the morphology of captive domesticated and feral mammals. Mammal Rev 35, 215–230.
Pavlicev, M., Cheverud, J.M., Wagner, G.P., 2010. Evolution of adaptive phenotypic variation patterns by direct selection for evolvability. Proc. R. Soc. B Biol. Sci. 278, 1903–1912.
Porto, A., de Oliveira, F.B., Shirai, L.T., de Conto, V., Marroig, G., 2009. The evolution of modularity in the mammalian skull I: Morphological integration patterns and magnitudes. Evol. Biol. 36, 118–135.
Porto, A., Shirai, L.T., de Oliveira, F.B., Marroig, G., 2013. Size variation, growth strategies, and the evolution of modularity in the mammalian skull. Evolution 67, 3305–3322.
Roach, N.T., Venkadesan, M., Rainbow, M.J., Lieberman, D.E., 2013. Elastic energy storage in the shoulder and the evolution of high-speed throwing in *Homo*. Nature 498, 483–486.
Rodman, P.S., 1979. Skeletal differentiation of *Macaca fascicularis* and *Macaca nemestrina*, in relation to arboreal and terrestrial quadrupedalism. Am. J. Phys. Anthropol. 51, 51–62.
Rolian, C., 2014. Genes, development, and evolvability in primate evolution. Evol. Anthropol. 23, 93–104.
Schmidt, M., Fischer, M.S., 2009. Morphological integration in mammalian limb proportions: Dissociation between function and development. Evolution 63, 749–766.
Sears, K.E., Capellini, T.D., Diogo, R., 2015. On the serial homology of the pectoral and pelvic girdles of tetrapods. Evolution 69, 2543–2555.
Selby, M., Lovejoy, C.O., 2017. Evolution of the hominoid scapula and its implications for earliest hominid locomotion. Am. J. Phys. Anthropol. 162, 682–700.
Shirai, L.T., Marroig, G., 2010. Skull modularity in neotropical marsupials and monkeys: Size variation and evolutionary constraint and flexibility. J. Exp. Zool. 314B, 663–683.
Simons, E.A., Frost, S.R., Harvati, K., McNulty, K., Singleton, M., 2020. Comparing rates of lineage diversification with rates of size and shape evolution in Catarrhine crania. Evol. Biol. 47, 153–163.
Sockol, M.D., Raichlen, D.A., Pontzer, H., 2007. Chimpanzee locomotor energetics and the origin of human bipedalism. Proc. Natl. Acad. Sci. USA 104, 12265–12269.
Tallman, M., 2013. Forelimb to hindlimb shape covariance in extant hominoids and fossil hominins. Anat. Rec. 296, 290–304.
Tuttle, R., Basmanjian, J.V., 1974. Electromyography of forearm musculature in *Gorilla* and problems related to knuckle-walking. Am. J. Phys. Anthropol. 37, 255–265.
Villmoare, B.A., Dunmore, C., Kilpatrick, S., Oertelt, N., Depew, M.J., Fish, J.L., 2014. Craniofacial modularity, character analysis, and the evolution of the premaxilla in early African hominins. J. Hum. Evol. 77, 143–154.
von Cramon-Taubadel, N., Frazier, B.C., Mirazon Lahr, M., 2007. The problem of assessing landmark error in geometric morphometrics: Theory, methods, and modifications. Am. J. Phys. Anthropol. 134, 24–35.
Wagner, G.P., 1984. On the eigenvalue distribution of genetic and phenotypic dispersion matrices: Evidence for a nonrandom organization of quantitative character variation. J. Math. Biol. 21, 77–95.
Young, N.M., 2003. A reassessment of living hominoid postcranial variability: Implications for ape evolution. J. Hum. Evol. 45, 441–464.
Young, N.M., 2006. Function, ontogeny and canalization of shape variance in the primate scapula. J. Anat. 209, 623–636.
Young, N.M., Wagner, G.P., Hallgrímsson, B., 2010. Development and the evolvability of human limbs. Proc. Natl. Acad. Sci. USA 107, 3400–3405.